UCRL-95909

Preprint

CONF-8706147--1

Cost Optimization of Induction Linac Drivers for Linear Colliders

William A. Barletta

December 29, 1986

For submission to:
Workshop on New Developments in Particle Acceleration Techniques,
Orsay, France, 29 June - 4 July 1987

Beam Research Program

Lawrence Livermore National Laboratory

Disclaimer

Cost Optimization of Induction Linac Drivers for Linear Colliders*

UCRL--95909

DE87 011560

William A. Barletta
University of California, Lawrence Livermore National Laboratory, Livermore, CA 94550, USA.

ABSTRACT

Recent developments in high reliability components for linear induction accelerators (LIA) make possible the use of these devices as economical power drives for very high gradient linear colliders. A particularly attractive realization of this "two-beam accelerator" approach is to configure the LIA as a monolithic relativistic klystron operating at 10 to 12 GHz with induction cells providing periodic reacceleration of the high current beam. Based upon a recent engineering design of a state-of-the-art, 10- to 20-MeV LIA at Lawrence Livermore National Laboratory, this paper presents an algorithm for scaling the cost of the relativistic klystron to the parameter regime of interest for the next generation high energy physics machines. The algorithm allows optimization of the collider luminosity with respect to cost by varying the characteristics (pulse length, drive current, repetition rate, etc.) of the klystron. It also allows us to explore cost sensitivities as a guide to research strategies for developing advanced accelerator technologies.

1. INTRODUCTION

The desire of high energy physicists to investigate phenomena at TeV energies has lead accelerator designers to consider new classes of machines that can achieve accelerating gradients >100 MeV/m in structures suitable for high repetition rate operation. The approach should be highly reliable and highly energy efficient if the costs of machine operation are to remain within currently acceptable bounds. In general, the accelerating gradient can be increased and the energy required per meter of accelerator structure reduced by scaling[1] the (effective) rf-structure of the accelerator to high frequencies (≥10 GHz.) The practical limits of this approach for conventional rf-cavities are set by the electron-induced breakdown limit and the surface heating limit, with little gain in gradient being achievable for frequencies exceeding 30 GHz. Considering that the cost of the rf-structure is likely to increase once it is miniaturized beyond a scale size of about 2 cm, we can select 10 to 30 GHz as the best frequency range for an advanced linear collider.

At the low end of this range we can employ many conventional klystrons to power the collider. More novel approaches, however, may offer the same performance at substantially lower cost. The two-beam accelerator (TBA) is a concept for using the high peak current beam produced with an linear induction accelerator (LIA) to excite an rf-generating structure at high frequency; the high peak power rf is then fed via a transfer structure to the miniaturized rf-cavities of the accelerator of the high energy beam. One variant of the TBA[2] employs a free-electron laser amplifier to transform the kinetic energy of the high current beam to high peak power microwaves. Another variant[3], more suitable to the frequency range from 10 to 15 GHz, converts the LIA into a monolithic relativistic klystron that runs the length of the high frequency rf-accelerator.

* Work performed jointly under the auspices of the U.S. Department of Energy by the Lawrence Livermore National Laboratory under contract No. W-7405-Eng-48 and for the Department of Defense; SDIO/BMD-ATC MIPR #W31-RPD-53-A127.

This paper describes a cost model developed to compare the relativistic klystron approach to powering a 12-GHz rf-accelerator with one powered by multiple klystrons. The considerations presented, however, are more general and can be used to estimate LIA costs over a wide range of operating parameters consistent with the constraints of beam dynamics and properties of materials. The scaling variables for the LIA include beam voltage (V), beam current (I), pulse length (T_p), repetition rate (f), and gradient (G) in the induction modules. The cost model is based upon the engineering design of a multistage, high repetition rate, induction linac (ETA II) now under construction at Lawrence Livermore National Laboratory (LLNL).

2. BASIS OF COST MODEL

The basis of any cost optimization study must be an accurate model of the scaling of accelerator cost with operating characteristics. The cost of LIAs is often assumed[1] to scale linearly with the number of volt-seconds in the accelerator cores; another frequently heard scaling is that LIAs cost $1 per volt. Although the cost algorithm developed below substantiates the rough linearity of cost with machine voltage, these and other rules of thumb can be grossly misleading. In particular, the cost per volt (C) can vary by nearly an order of magnitude depending upon the actual operating specifications of the accelerator.

2.1. General Considerations

The cost analysis begins with the division of the LIA into its primary subsystems: an induction-driven injector, the accelerator cells, beam transport, and ancillary systems.

$$C_{accel} = C_{inj} + C_{cell} + C_{tran} + C_{sys} \ . \tag{1}$$

The injector and accelerator cells consist of nonresonant, axisymmetric gap structures that enclose toroidal cores of ferrimagnetic material. A drive voltage impressed across the gap by the power drive changes the flux in the core, inducing an axial electric field that accelerates the electrons. In general, the electron injector and accelerator cells have similar power drive networks (Fig. 1): a dc-power supply charges a set of intermediate storage capacitors via a command resonant charging circuit. These intermediate stores are discharged through the primary commutators--thyratrons (or SCRs)--into low impedance magnetic pulse compressors (MAG).[4] Each compressor can power a number of accelerator cells connected in parallel. Although the high current beam (~1kA) forms the primary load for the pulse compressors, a parallel compensation network maintains a constant accelerating voltage throughout the beam pulse. The fundamental limits to the operating characteristics of the LIA are set by beam transport physics, material properties, and primary commutator recovery times.[5]

The injector scaling assumes a gridless, constant perveance design with space charge limited emission, i.e., the injector voltage (V_{inj}) is given by

$$V_{inj} = k\,(I_{beam})^{2/3} \ , \tag{2}$$

where V_{inj} is in MeV, I_{beam} is in kA, and $k = 0.75$ (1.45) for high current (brightness) beams. The scaled designs employ a thermionic (dispenser) cathode. The primary cost components include the injector induction structure, focusing, MAG drives, intermediate stores and power supplies, alignment fixtures, and vacuum.

Ancillary systems include vacuum and gas handling systems, low and extremely low conductivity water (LCW), electrical fluids such as insulating fluids and compensation loads, alignment fixtures, miscellaneous fixtures and structures, and instrumentation and controls. Based

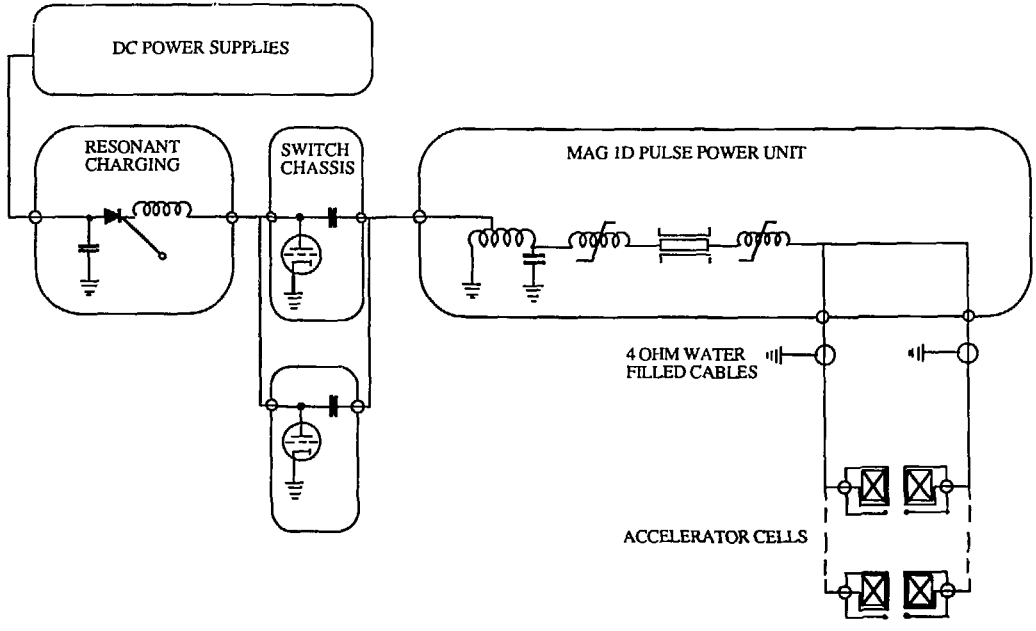

Figure 1. Schematic of baseline design of induction linac.

on review of a detailed installation schedule, we find that the cost of installation, support engineering, and its associated supplies and expenses is each a nearly constant percentage of the hardware cost (~10%) . The actual percentage will depend upon the labor rate at the accelerator site. Separate support facilities are not included, i.e., the hardware cost assumes an existing technical infrastructure in the vicinity of the accelerator site.

2.2. Accelerator Cell and Drive Design

The basis for scaling the design of the accelerator cells and drives is the prototype of the ETA II cell, illustrated in Fig. 2, the MAG-1D[6] pulse compressor, and its associated thyratron-switched intermediate stores. The most important cell characteristics are the gap width (w), the inner radius of the cell (r_i), the radius of the bean pipe (b), and the volt-seconds of core material. The cores consist of toroids of ferrite (TDK PE-11), which has minimal core losses for short saturation times (<1 μs). The gap size and shape is selected to minimize the Q of the cell and the coupling (Z) of the beam to transverse (beam breakup) modes of the cell. The baseline design has a gap width (w) of 0.635 cm for a conservatively chosen gap field stress (E_g) of 175 kV/cm. The insulator, which separates the vacuum from the insulating fluid (FC-75), is set at an angle such that all TM cavity modes will pass through the insulator without reflection to be absorbed by the ferrite. The slight reentrant design of the gap shields the insulator from stray beam electrons. The difference between the pipe size and inner cell radius (≈2 cm) is accounted for by the size of steering magnets and focusing magnets (about 1 to 3 kG) and spacers to allow insulating fluid to flow along the inner boundaries of the ferrite.

The choice of inner radius (7.5 cm) for the baseline design was set to keep the beam breakup (BBU) growth below 10 in an accelerator for a mono-energetic, 3-kA beam transported with quadrupoles through ~10^3 gaps (accelerating cavities). With such a focusing system, the beam breakup growth (S) will scale as

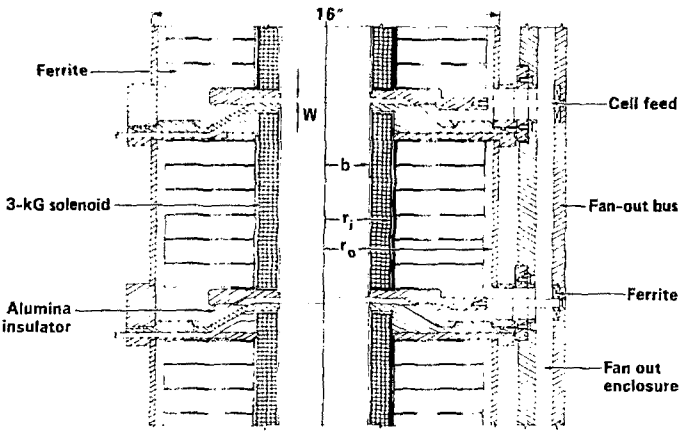

Figure 2. Cross-section of a typical low-gamma 10-cell module of the new 150-kV accelerator cell.

$$S \propto I_{beam} (w/b^2) (\ln N_g) \, \mathrm{Im}\, P_1(\omega) / B E_g \ , \tag{3}$$

where N_g is the number of gaps and B is the (effective) field strength of the magnetic transport. Typically, we can replace b in Eq. (3) with r_i for the purpose of scaling costs. The quantity $\mathrm{Im}\, P_1(\omega)$ is that part of the cavity response function that produces growth of TM_{1n0} beam breakup modes. To suppress BBU we minimize $|\, \mathrm{Im}\, P_1(\omega)\,|$ by arranging that the beam induced fields in the cavity are purely outgoing. That is, we shape the gap so as to approximate a perfectly matched radial line. In that case,[7] $|\, \mathrm{Im}\, P_1(\omega)\,|$ is a slowly varying value of w/b and is roughly linear over the range $0.1 < w/b < 1$;

$$|\, \mathrm{Im}\, P_1(\omega)\,| \approx 0.71 - 0.33\, w/b \ . \tag{4}$$

Typically, in LIAs built to date, b is several centimeters, and $w/b \approx 0.3$. In contrast, the relativistic klystron variant of the TBA will require a pipe size < 1 cm (beyond cutoff), in which case $w/b > 1$. Two factors suppress the BBU in this case: For the accelerator cells, $w/b \approx 3$, at which value $|\, \mathrm{Im}\, P_1(\omega)\,|$ is of order 10^{-2}. However, the BBU growth due to the beam interaction with the klystron cavity is rapid. Almost as rapid is the growth of transverse motion due to the resistive wall instability.[8] Fortunately, the large spread in the beam's betatron frequency due to the large energy spread induced by the klystron action and/or by laser-guided transport[7] allows shrinking the pipe size below cut-off ($r_i = 2.5$ cm) as is required for the operation of the klystron.

The outer radius of the cell is determined by the accelerating voltage (V_{acc}) and the cell length (z) via the magnetic induction equation,

$$V_{acc}\, T_p = A\, (\Delta B) \ , \tag{5}$$

where A is the cross-sectional area of the ferrite, ΔB is the total flux swing (0.6 Wb/m^2), and T_p is the pulse duration. Writing the cell length (z) in terms of the effective gradient (G) and the packing fraction for the ferrites (p) we can recast Eq. (5) as

$$r_o = r_i + (G\, T_p / p) / \Delta B \ . \tag{6}$$

Typically, the packing fraction is 0.8. The effective gradient (G) for the baseline design is 0.75 MeV/m.

For ease in designing the beam transport system, it is necessary that the waveform of the accelerating voltage vary by no more than 1% over time. In that case the length of the cell and the properties of the ferromagnetic material are subject to an additional constraint. The region between the high voltage drive blade and the back wall of the induction cavity should be designed to be a constant impedance transmission line loaded with a high μ material to slow the wave speed. Even if the transverse dimension of the cavity is sufficiently large to avoid a saturation wave forming in the core, the transit time in the longitudinal direction must equal or exceed the pulse length. That is,

$$z \geq T_p\, (\mu\varepsilon)^{1/2} \ . \tag{7}$$

Moreover, the requirement that the transmission line have a constant impedance dictates that the core must be composed of a material like ferrite rather than wound metallic glass tapes. For high fidelity ferrites

$$(\mu\varepsilon)^{1/2} \approx 100 \ ; \tag{8}$$

hence, Eq. (5) can be written as

$$c(r_o-r_i) / (\mu\varepsilon)^{1/2} \geq (V/\Delta B) \ . \qquad (9)$$

If the core geometry is such that the value of the magnetic field in the core varies inversely with radius, then, to avoid saturation anywhere in the core, Eq. (9) should be modified to

$$c(r_o-r_i) / (\mu\varepsilon)^{1/2} \geq [\ln (r_o/r_i)] (V/\Delta B) \ . \qquad (10)$$

For both compactness and convenience in installation and maintenance, the accelerator cells are packaged in blocks of ten. Each block of cells is attached to a strongback structure, which is the primary means of assuring accelerator alignment to better than 0.5 mm. If the beam transport is provided by a laser-ionized channel or if the energy spread in the beam is large, as in the case of the relativistic klystron, the structural demands on the strongback are eased considerably, because the cell blocks are shorter and lighter.

The constraint to minimize operating costs of high luminosity linear colliders requires us to keep core magnetization (hysteresis) losses small. The same design consideration allows us to minimize beam energy variations during the pulse ($\Delta E/E < 1\%$). In practical terms, the magnetization current should not exceed 20% of the beam current, i.e.,

$$I_m = (1/L) \int V_{acc}\, dt \leq 0.2\, I_{beam} \ , \qquad (11)$$

where the core inductance (L) is given by

$$L = (\mu/2\pi)\, z \ln (r_o/r_i) \ . \qquad (12)$$

Then, the core loss (joules per volt) is

$$\mathfrak{R} = (\pi/\mu)\, G\, T_p^2\, (\ln r_o/r_i)^{-1} \ . \qquad (13)$$

For the baseline design of the core $T_p = 75$ ns and $\mathfrak{R} = 16$ J/MV; reducing T_p to 50 ns would reduce $\mathfrak{R}$ to < 9 J/MV. For relativistic klystrons designed to power large linear colliders (~4 GV of induction cells per TeV of high energy linac), the incentives to lower T_p are clear.

The accelerator cells are driven by Freon-cooled MAG-1Ds (Fig. 3) that consist of metallic glass, nonlinear inductors that operate from the unsaturated to fully saturated state in the pulse compression process. For linear colliders operating at repetition rates between 100 to 1000 Hz, the MAG-1D pulse compressors are capable of continuous operation[5] and have been tested for hundreds of millions of pulses without change in operating characteristics. The cost model assumes that the thyratron switches used in the intermediate stores are ceramic envelope tubes (by English Electric Valve Corp.) capable of continuous 1-kHz operation. For collider operation at 100 to 200 Hz, glass envelope tubes (from multiple manufacturers) could be used with a cost savings of about a factor of three.

3. COST SCALING RELATIONS

3.1 Scaling Principles

By breaking down each subsystem into a set of components and their internal constituents (if necessary), we can arrive at a descriptive level at which scaling relations can be assigned on the basis of basic physical characteristics. For example, the cost of the accelerator cell housing is

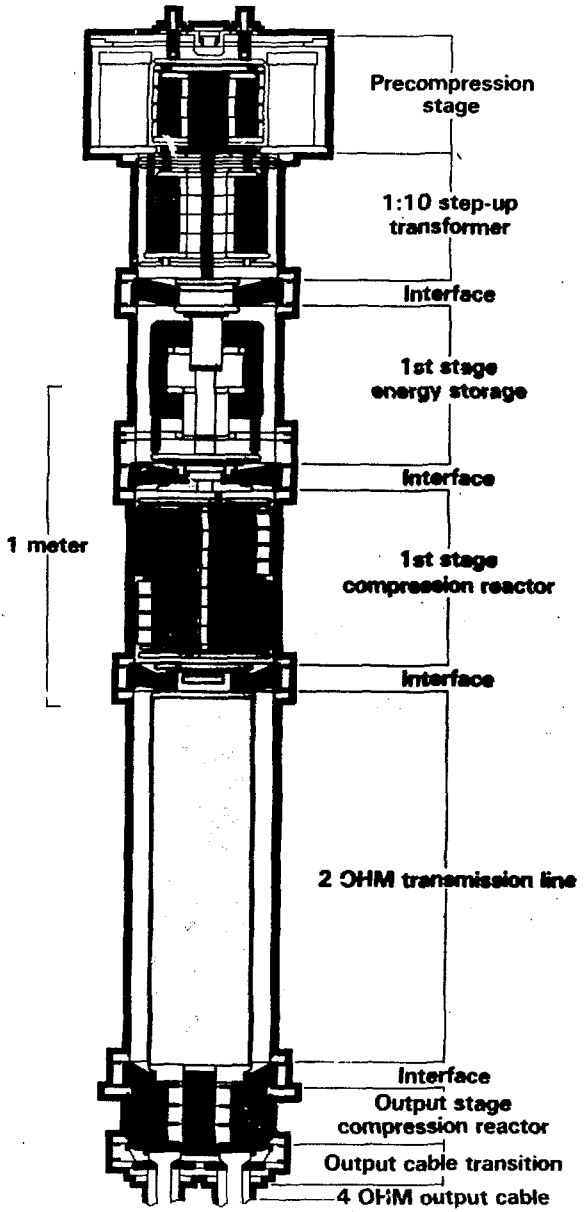

Figure 3. Cutaway view of MAG-1D.

determined by the quantity of metal and, more significantly, by the length of machining, finishing and welding time involved in the cell manufacture. This time scales linearly with the surface area to be machined, finished, welded, and inspected. The baseline cost estimate includes no reduction for the use of production engineering techniques, such as large scale metal casting and robot welding. Such techniques might reduce the cost of the accelerator cell housings by more than 30%. A complete set of components, internals, and scaling determinants of the accelerator subsystem are listed in Table 1.

In similar fashion, we can assign scaling determinants to the components included among the ancillary systems. These characteristics, listed in Table 2, require some qualifying comments: As the cell size decreases, the vacuum system will become conductance limited rather than pumping speed limited. Consequently, the system cost will then scale with machine length rather than with the pumping volume. Over the range of accelerator sizes of interest for linear colliders, the cost of the instrumentation and control system is assumed to be a "buy-in" fixed cost plus a percentage of the accelerator cell costs.

Table 1.

Scaling principles for accelerator cell components.

Component	Internals	Scaling
Power Supplies	DC supplies CRCs	Average Power
Intermediate stores	Capacitors Thyratrons	Pulse energy Average current, pulse energy
Magnetic compressors	MAG-1D	Pulse energy
Accelerator cells	Ferrites Cell housing, gap	Volume (V_{acc}, T, G) Surface area (r_i, r_o, G) Total voltage
Strongback		Cell weight and length

Table 2.

Cost scaling determinants for ancillary systems.

Component	Scaling
LCW and ELCW	Pulse energy, average power
Vacuum	Pumping volume
Insulating fluids	Average power
Fixtures and Alignment	Length
Instrumentation and Controls	System complexity
Beam dump	Average power into dump

The injector subsystem consists of a collection of components similar to those of the accelerating cells. In addition, the injector includes some separate ancillaries such as vacuum, focusing, and alignment fixtures. The subsystem is characterized by an anode-cathode voltage (V_{inj}), which is related to the beam current by Eq. (2). The scaling of the cost of the injector follows from the same physical considerations as for the accelerator cells.

The most complex scaling applies to the beam transport system as several alternative focusing schemes are possible:

a) continuous solenoid,

b) solenoids in the first 20 MeV followed by a quadrupole lattice, and

c) laser guiding.

The guiding principle in the specification of the transport system is that the BBU growth parameter (S) in Eq. (3) is kept constant. Equation (3), however, assumes a mono-energetic beam with uniform betatron frequency(k_β). Consequently, scaling the transport schemes is complicated by the degree of energy spread, $C = (\Delta E/E)$, of the electron beam. For the relativistic klystron, $C \leq 1\%$ for the first 15 to 40 MeV of induction modules; following the klystron cavity interaction, C increases to about 50%. With such a large energy spread, the betatron frequency spread for the beam will be sufficiently large that the phase mixing of the beam is more rapid than the maximum possible BBU growth rate. That is, the transverse mode for a 3-kA beam will actually damp even for r_0 as small as 2.5 cm if the solenoidal field is kept constant throughout the accelerator at 3 kG, the value for the baseline linac design. Therefore, the cost of powering the continuous solenoidal transport can be scaled in proportion to the total field volume and the square of the beam current. The cost of the magnet windings is proportional to the accelerator length, the current, and the inner radius r_i.

For induction linacs designed for other applications, BBU constraints may be relaxed, or they may be combined with other constraints on the transport system such as the reduction of corkscrewing of the beam.[7] In such alternate cases the optimum transport strategy may require the variation of B with the beam energy. Then the scaling relation should be recast in terms of an appropriate average value of the magnetic field.

The use of a quadrupole lattice between the accelerating cells will reduce the average gradient in the induction linac by as much as 50%. This consideration alone makes the use of solenoids in the first 20 MeV followed by a quadrupole lattice (scheme b above) relatively uninteresting for the driver of a linear collider.

Laser guiding[9] (scheme c above) introduces a number of design elements foreign to all linacs save one--the Advanced Test Accelerator (ATA). This technique, used daily to transport high current beams through the ATA, may reduce the cost of the transport in the induction linac by an order of magnitude. The transport components in this approach are a very low angular jitter, near-diffraction-limited, repetition-rated KrF laser (≈1 J per pulse in ≈20 ns), a gas handling system to maintain a partial pressure of $\approx 10^{-4}$ Torr of benzene, and magnetic transition sections to match the electron beam onto (and off of) the laser-ionized gas channel. For repetition rates ≤250 Hz, suitable KrF lasers are available commercially. Diffraction will eventually reduce the laser fluence below the level needed ($<0.2\ J/cm^2$) to ionize a suitably large fraction of the benzene; therefore, a new laser beam must be reintroduced into the linac every ≈125 m. The beamline must have periodic chicanes with differential pumping and matching magnets to accommodate introduction of the laser pulse . For this scheme, cost will scale in proportion to the length of the linac.

In addition to the focusing components discussed above, all schemes with magnetic transport must include steering magnets at periodic intervals, the length of which is determined by alignment requirements. All transport schemes require a matching section between the injector output and the main accelerator transport.

3.2. Scaling Equations

Variables to be used in the scaling equations include the total accelerating voltage (V) in MV, the the total volt-seconds of core ($W = V T_p$), the gap stress (E_g) in kV/cm, the single pulse energy ($E = V I_{beam} T_p$) in joules, the average power ($P = f E$) in MW, the effective gradient (G) in MV/m, and the inner radius (r_i) in cm. In the scaling equations italicized quantities refer to injector voltage, power, pulse energy, etc. Costs are specified in constant FY87 thousands of dollars.

3.2.1 Injector Subsystem

The scaling equation for the injector is divided into five separate components:

$$C_{inj} = [724\ (\ W / 0.17)]_{cells} + [475\ (E / 450)]_{mag} + [450\ (P / 2.25)]_{isps} + [165\ (V / 3)^3\ ]_{vac} + [60\ ]_{align}\ . \qquad (14)$$

As each arm of the linear collider is driven by a separate induction linac, this injector cost must be doubled in the estimate of total hardware cost. For most variants of the two-beam accelerator approach this cost is a small fraction of the total.

3.2.2 Beam Transport Subsystems

For solenoidal transport, the cost has three separate components:

$$C_{sol} = [(57 + 81\ (r_i/7.5)\ (I/3000)\ )\ (V/1.5)\ (I/3000)\ (r_i/7.5)\ (0.75/G)]_{focus} + [42\ (V/1.5)\ (r_i/7.5)\ (0.75/G)]_{steer} + [\ 78\ ]_{match}\ . \qquad (15)$$

For the alternative laser guiding scheme the scaling equation is

$$C_{laser} = 7.5\ V\ G^{-1}\ , \qquad (16)$$

which includes laser, gas handling, and matching magnet costs for $f \leq 250$ Hz.

3.2.3. Accelerator Cell Subsystems

The cell block cost is

$$C_{block} = 234\ (V / 1.5)\ (r_o / 20)^2\ (0.75 / G)\ (175 / E_g)\ , \qquad (17)$$

where r_o is related to r_i by Eq. (6). The ferrite cost is given by

$$C_{ferrite} = 44\ (\ W / 0.225)\ [(r_o + r_i\ ) / 27.5]\ . \qquad (18)$$

where we have used the relation between the area and volume of the ferrite, $Vol = \pi\ A\ (r_o + r_i)$. The cost of intermediate stores and power supplies scales as

$$C_{isps} = 698\ (P / 3.2) + 5\ (E / 630)\ . \qquad (19)$$

The scaling for the magnetic pulse compressors is

$$C_{mag} = 241\ (E / 630)\ . \qquad (20)$$

For power systems delivering pulses at repetition rates ≈100 Hz the magnetic modulators and intermediate stores can be reengineered to reduce costs by nearly a factor of two. The cost of the strongback alignment structure is

$$C_{strong} = 450\,(V / 12.5)\,(r_o / 20)^2\,(0.75 / G)\,K\ , \tag{21}$$

where the constant K depends on the focusing scheme; namely,

$$\begin{aligned} K &= 1.0 \text{ for quadrupoles,} \\ &= 0.6 \text{ for solenoids,} \\ &= 0.5 \text{ for laser guiding.} \end{aligned} \tag{22}$$

3.2.4. Ancillary Subsystems

The cost for low and extremely low conductivity water will scale as

$$C_{lcw} = 90\,(P / 13.1)\ , \tag{23}$$

for $f > 100$ Hz. For $f < 100$ Hz we should use the value of C_{lcw} at $f = 100$ Hz. The vacuum system is scaled as if it were pumping-speed limited (valid for $r_i \geq 2.5$ cm):

$$C_{vac} = 660\,(V / 12.5)\,(r_i / 7.5)^2\,(0.75 / G)\,K\ . \tag{24}$$

where K is given by Eq. (22). The cost of electrical fluids is proportional to average beam power;

$$C_{fluid} = 542\,(P / 13.1)\ . \tag{25}$$

The scaling of dump costs is similar to that for reactors, i.e., \$1 per watt of beam power into the dump (P_d). For the relativistic klystron, we assume that the average beam voltage at the dump (V_d) is 35 MeV, hence, $P_d = V_d\,T_p\,I_{beam}\,f$

The collider, therefore, has two dumps of cost,

$$C_{dump} = 1000\,P_d\ . \tag{26}$$

The cost of fixtures is proportional to the length of the induction linac;

$$C_{fixture} = 20\,(V / 12.5)\,(0.75 / G)\ . \tag{27}$$

The cost of the instruments and controls scales as a fixed value plus a percentage of the cost of the hardware to be monitored and controlled;

$$C_{i\&c} \approx 3000 + 0.04\,(C_{inj} + C_{cell} + C_{focus})\ . \tag{28}$$

Summing the cost equations ((14) through (21), and (23) through (28)) yields the total hardware cost for the induction linac driver.

3.2.5 Installation and Engineering Support

The installation costs for the base design were estimated on a component by component basis; for estimating purposes the installation costs can be taken as a fixed percentage of the total hardware costs adjusted to the fully-loaded labor rate (R) in \$K/man-month.

$$C_{install} = 0.09\, C_{hardware}\, (R / 10)\ . \qquad (29)$$

Similarly, a cost for engineering management and support is estimated as a percentage of the hardware costs, i.e.,

$$C_{engin} = 0.125\, C_{hardware}\ . \qquad (30)$$

Supplies and equipment used for engineering and installation increases the total cost by 10% ;

$$C_{s\&e} = 0.1\, C_{hardware} \qquad (31)$$

Adding these installation costs to the hardware cost yields a total cost that includes ≈10% contingency distributed (unevenly) among the various cost centers.

4. APPLICATION OF THE SCALING ALGORITHM

4.1. Driver Cost for a Linear Collider

The scaling algorithm developed in the preceding section can be applied to estimate the hardware costs of the induction linac driver for a high luminosity, 400 GeV-on-400 GeV linear collider described in Ref. 3. The induction driver is configured as a relativistic klystron producing 1.4 GW/m of ≈11.4 GHz rf power. The results, given in Table 3, use the baseline values for those component characteristics not specified. The total hardware cost, $483M, translates to 10^{-4} $/rf-watt, which is much smaller than the cost of rf power delivered by conventional klystrons (10^{-2} $/rf-watt), and which compares quite favorably with earlier estimates[2] of the requirements to make high gradient colliders practical. Moreover, if the anticipated savings from using standard production engineering techniques can be realized, the hardware costs can be reduced by 25%.

4.2. Cost Sensitivities and Optimization

Having obtained encouraging results from this initial estimate, we can proceed to use the scaling relations to study the sensitivity of driver cost to its design characteristics. The rationale for sensitivity studies is to suggest how we might optimize the specification of the driver for the linear collider. One way to proceed is vary the induction driver specifications so as to maximize the collider luminosity per unit capital cost. An alternative would be to formulate a measure that accounts for both capital and operating cost, and then maximize the luminosity per unit measure.

Three examples of the cost sensitivities indicate the directions offered by the first approach. Figures 4, 5, and 6 show the variation of driver cost per volt with pulse length, gradient, and repetition rate, respectively. For constant gradient designs the costs are seen to rise quadratically with pulse length. At constant pulse length the costs rise quadratically with gradient. Lowering the reference design value from 60 ns to 50 ns would reduce driver costs by greater than 22%, assuming that the voltage rise time can be shortened in proportion to the pulse length. This assumption is valid for $30 \le T_p \le 80$ ns. For the driver to provide the same power per unit length to the rf-structure, the induction linac voltage (and gradient) would have to rise by 12%. The number of rf feed lines would have to increase. As these feed lines are inexpensive, we should expect this optimization approach to realize a net savings of ≈5% (≈$25M) over the estimate of Table 3. A different tack might be to increase the current to compensate for the shorter pulse length. In that case, the savings should exceed $50M.

Table 3.

Induction linac cost for relativistic klystron driver of linear collider.

Subsystem	Component	Cost ($K)	Totals ($K)	*Production engineered*
Injector	injector (2)	1,363	1,363	
Transport	laser guide	19,688	19,688	
Accelerator cells	cell blocks	230,344		*161,241*
	ferrites	26,133		
	MAG-1D	131,211		
	i.s. and p.s.	11,776		
	strongback	26,578		*18,605*
			426,042	*322,832*
Ancillary systems	Vacuum	9,240		
	Fixture and Align	4,200		
	LCW	303		
	Elec. fluids	1,825		
	I & C	19,820		
	Dump (2)	81		
			35,468	
Total components			482,561	*379,351*
Install			43,430	*34,142*
Engineering support			60,320	*47,419*
S & E			48,256	*37,935*
TOTAL (as of 12/24/86)			634,567	*498,846*

Accelerator Specifications

Voltage (MV)	3500	Grad (MV/m)	1
Current (A)	1750	Radius-inner (cm)	2.5
Pulse (ns)	60	Radius-outer (cm)	15.00
Frequency (Hz)	120	Packing	0.8

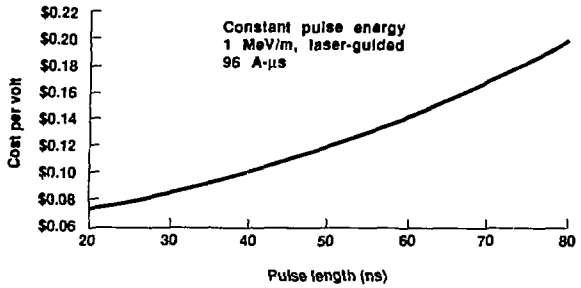

Figure 4. Induction driver cost vs pulse length.

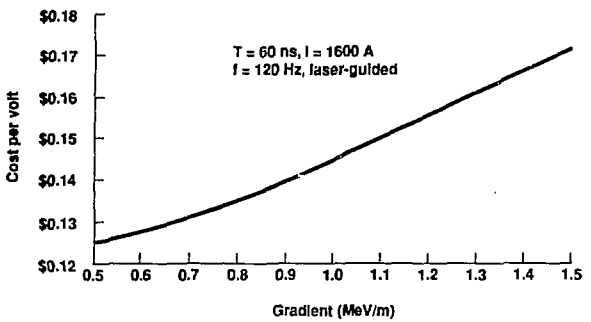

Figure 5. Driver cost vs gradient.

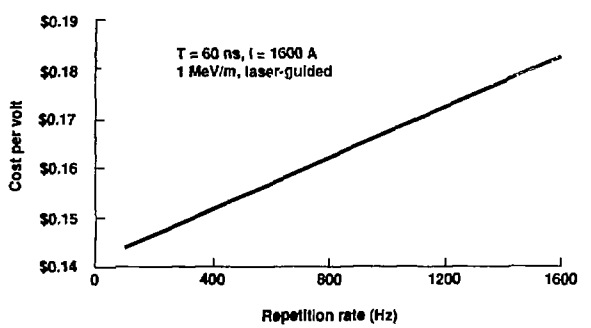

Figure 6. Driver cost vs repetition frequency.

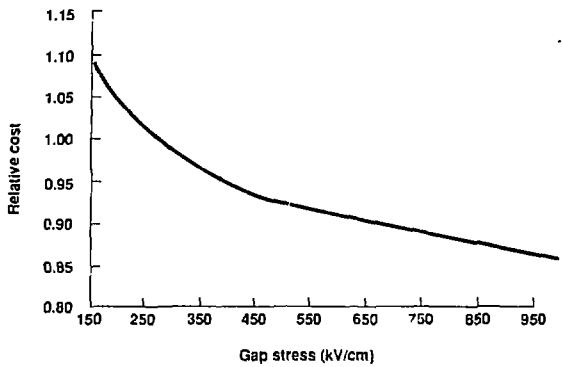

Figure 7. Relative costs vs gap stress.

The electrical power requirements for the reference collider design (at 120 Hz) are 60 MW. If the allowed power consumption is 120 MW, the luminosity of the collider can be doubled at a less than 1% increase in the capital cost by designing the driver to operate at 240 Hz.

Finally, a plot of relative cost vs E_g (Fig. 7) shows the impact in advancing pulsed-power technology so that the electrical stress in the accelerating gap can be increased from the baseline value of 175 kV/cm. Doubling the allowed stress would reduced the driver cost by ≈10%.

5. CONCLUSIONS

The costs of induction linacs can be estimated over a wide range of operating specifications relevant to driving large linear colliders. The estimates, based on scaling the costs of the ETA II now under construction at LLNL, show that the relativistic klystron has the potential to produce rf-power at $<10^{-5}$ \$/rf-watt. This value is both strongly cost-competitive with conventional means of powering rf-structures at frequencies about 10 to 20 GHz and is sufficiently low to make practical high gradient linear colliders with TeV center of mass energies. Initial cost sensitivity studies indicate that the driver characteristics can be optimized to reduce costs at least an additional 20%.

* * *

REFERENCES

1) R.A. Jameson, "New Linac Technology for SSC and Beyond", in *Proc. 12th International Conf. on High Energy Accelerators, FERMILAB, Aug. 11-13, 1983, pp. 497 -50.*

2) D.B. Hopkins, A.M. Sessler, and J.S. Wurtele, "The Two-Beam Accelerator," *Nuc. Inst. & Meth. for Phys. Res.*, **228**, pp. 15-19 (1984).

3) S.S. Yu and A.M. Sessler, *The Relativistic Klystron Two-Beam Accelerator*, Lawrence Livermore National Laboratory, Livermore, CA., UCRL-96083 (1987), submitted to *Phys. Rev. Lett.*

4) D. Birx, "The Applications of Magnetic Switches as Pulse Sources for Induction Linacs", *IEEE Transactions in Nuclear Science*, NS-30, 4, Aug., 1983.

5) D.L. Birx, G.J. Caporaso, L.L. Reginato, *Linear Induction Accelerator Parameter Options*, Lawrence Livermore National Laboratory, Livermore, CA, UCID-20786 (1986).

6) D.L. Birx, *A Collection of Thoughts on the Optimization of Magnetically Driven Induction Linacs for the Purpose of Radiation Processing,*, Lawrence Livermore National Laboratory, Livermore, CA, UCRL-92828 (1985).

7) G.J. Caporaso, "Control of Beam Dynamics in High Energy Induction Linacs," in *Proc. of LINAC '86 Conference, SLAC*, July, 1986.

8) G.J. Caporaso, W.A. Barletta, and V.K. Neil, "Transverse Resistive Wall Instability of a Relativistic Electron Beam," *Particle Accelerators*, 11, pp. 71-79, (1980).

9) G.J. Caporaso, "Laser Guiding of Electron Beams in the Advanced Test Accelerator," *Phys. Rev. Lett.*, 57, 13, (1986).